### Title

3D Harmonic and Subharmonic Imaging for Characterizing Breast Lesions: A Multi-Center Clinical Trial.




### Journal

Journal of Ultrasound in Medicine, 41(7)



### Authors

Forsberg, Flemming

Piccoli, Catherine

Sridharan, Anush

et al.



### Publication Date

2022-07-01

### DOI

10.1002/jum.15848

Peer reviewed

HHS Public Access

Author manuscript

*J Ultrasound Med*. Author manuscript; available in PMC 2023 January 29.

Published in final edited form as:

*J Ultrasound Med*. 2022 July ; 41(7): 1667–1675. doi:10.1002/jum.15848.

# 3D Harmonic and Subharmonic Imaging for Characterizing Breast Lesions:

## A Multi-Center Clinical Trial

**Flemming Forsberg, PhD**,
Department of Radiology, Thomas Jefferson University, Philadelphia, PA, USA

**Catherine W. Piccoli, MD**,
South Jersey Radiology, Voorhees, NJ, USA

**Anush Sridharan, PhD**,
Department of Radiology, Thomas Jefferson University, Philadelphia, PA, USA; Department of Electrical and Computer Engineering, Drexel University, Philadelphia, PA, USA

**Annina Wilkes, MD**,
Department of Radiology, Thomas Jefferson University, Philadelphia, PA, USA

**Alexander Sevrukov, MD**,
Department of Radiology, Thomas Jefferson University, Philadelphia, PA, USA

**Haydee Ojeda-Fournier, MD**,
Department of Radiology, University of California San Diego, San Diego, CA, USA

**Robert F. Mattrey, MD**,
Department of Radiology, University of California San Diego, San Diego, CA, USA

**Priscilla Machado, MD**,
Department of Radiology, Thomas Jefferson University, Philadelphia, PA, USA

**Maria Stanczak, RDMS, MS**,
Department of Radiology, Thomas Jefferson University, Philadelphia, PA, USA

**Daniel A. Merton, RDMS**,
Department of Radiology, Thomas Jefferson University, Philadelphia, PA, USA

**Kirk Wallace, PhD**,
GE Global Research, Niskayuna, NY, USA

**John R. Eisenbrey, PhD**
Department of Radiology, Thomas Jefferson University, Philadelphia, PA, USA

## Abstract

Address correspondence to Flemming Forsberg, PhD, FAIUM, FAIMBE, Department of Radiology, 763H Main Building, Thomas Jefferson University, 132 South 10th Street, Philadelphia, PA 19107, USA, flemming.forsberg@jefferson.edu.

**Objective—**Breast cancer is the most frequent type of cancer among women. This multi-center study assessed the ability of 3D contrast-enhanced ultrasound to characterize suspicious breast lesions using clinical assessments and quantitative parameters.

**Methods—**Women with suspicious breast lesions scheduled for biopsy were enrolled in this prospective, study. Following 2D grayscale ultrasound and power Doppler imaging (PDI), a contrast agent (Definity; Lantheus) was administrated. Contrast-enhanced 3D harmonic imaging (HI; transmitting/receiving at 5.0/10.0 MHz), as well as 3D subharmonic imaging (SHI; transmitting/receiving at 5.8/2.9 MHz), were performed using a modified Logiq 9 scanner (GE Healthcare). Five radiologists independently scored the imaging modes (including standard-of-care imaging) using a 7-point BIRADS scale as well as lesion vascularity and diagnostic confidence. Parametric volumes were constructed from time-intensity curves for vascular heterogeneity, perfusion, and area under the curve. Diagnostic accuracy was determined relative to pathology using receiver operating characteristic (ROC) and reverse, step-wise logistical regression analyses. The κ-statistic was calculated for inter-reader agreement.

**Results—**Data were successfully acquired in 219 cases and biopsies indicated 164 (75%) benign and 55 (25%) malignant lesions. SHI depicted more anastomoses and vascularity than HI ($P <$ .021), but there were no differences by pathology ($P >$ .27). Ultrasound achieved accuracies of 82 to 85%, which was significantly better than standard-of-care imaging (72%; $P <$ .03). SHI increased diagnostic confidence by 3 to 6% ($P <$ .05), but inter-reader agreements were medium to low ($\kappa < 0.52$). The best regression model achieved 97% accuracy by combining clinical reads and parametric SHI.

**Conclusions—**Combining quantitative 3D SHI parameters and clinical assessments improves the characterization of suspicious breast lesions.

## Keywords

3D ultrasound imaging; breast cancer; contrast-enhanced ultrasound; harmonic imaging; subharmonic imaging

Breast cancer is the second most common cancer in the world and the most frequent type of cancer among women (approximately 30% of all cancers) with an estimated 281,550 new cases expected in the United States alone in 2021.[1,2] Moreover, breast cancer accounts for 15% of all cancer deaths in women in America making it the second leading cause of cancer mortality. Detecting breast cancer by as little as 3 months earlier can yield better treatment outcomes.[3,4] In the United States, mammography is the primary imaging modality for breast cancer screening. However, the sensitivity of mammography decreases to around 48 to 64% in younger patients (<50 years old) and in patients with dense breasts.[4] Hence, ultrasound imaging, as an adjunct to mammography, becomes a cost-effective and patient-friendly alternative for both screening and diagnosis.[4,5]

The sensitivity and specificity of ultrasound imaging can be improved by intravenous (IV) injection of encapsulated, gas-filled microbubbles (typically <8 μm in diameter) as vascular contrast agents.[5-7] These contrast agents can produce signal enhancement of up to 30 dB and have been shown to provide a noninvasive measure of breast tumor neovascularity corresponding to vessels 20 to 39 μm in diameter.[6,7] At higher incident acoustic pressures

(>200 kPa), these microbubbles oscillate nonlinearly over a wide range of frequencies from subharmonics ($f_0/2$) to second harmonics ($2f_0$) and ultraharmonics ($3f_0/2$) of the insonation frequency ($f_0$) as well as its multiples. These signals can be used to create contrast-specific imaging modes, such as subharmonic imaging (SHI), harmonic imaging (HI), and superharmonic imaging, respectively.[6] Most state-of-the-art ultrasound scanners provide HI, and more recently, SHI has also become commercially available.[8]

The utility of SHI has been studied and validated *in vitro* as well as *in vivo* by many independent groups.[9-22] The first human study of SHI was a pilot study of 14 women with breast lesions scheduled for a subsequent biopsy.[13-15] Results showed that SHI had the highest accuracy compared to regular grayscale, Doppler, and mammography with receiver operating characteristic (ROC) analysis producing an area under the curve ($A_z$) of 0.78, which improved to 0.90 after image processing.[13,14] Based on these encouraging results, the use of quantitative biomarkers derived from 3D SHI for characterization of breast lesions was investigated in a larger cohort of patients.[21,22] These SHI biomarkers achieved $A_z$ values from 0.52 to 0.75 based on analyzing 83 lesions, while the best logistical regression model reached an $A_z$ of 0.90.[22]

Hence, this prospective, multi-center study assessed the ability of 3D HI and SHI to characterize suspicious breast lesions using clinical assessments on their own and combined with the above-mentioned quantitative parameters. Results were compared to conventional ultrasound and mammography, using pathology as the reference standard.

## Materials and Methods

### Study Population

Adult women (≥21 years old) scheduled for a clinically indicated biopsy of an indeterminate breast lesion (or abnormal area) based on standard of care (SoC) imaging (mammography and/or grayscale ultrasound) were enrolled in this IRB-approved multi-center clinical study after providing written informed consent. Complete inclusion and exclusion criteria are provided in Table 1. The study was conducted between January 2011 and December 2015 at Thomas Jefferson University (TJU) and University of California–San Diego (UCSD), while data analysis was completed by June 2019. The study was carried out under a Food and Drug Administration (FDA) approved IND (# 112,241) and registered with ClinicalTrials.gov (NCT01490892).

### Ultrasound Contrast Agent

This study used perflutren lipid microspheres (Definity®; Lantheus Medical Imaging Inc., N Billerica, MA) as the ultrasound contrast agent.[6,23] Per the manufacturers' recommendations, the Definity vials were warmed to room temperature and mixed for 45 seconds using a VIALMIX (Lantheus Medical Imaging). After this activation, each vial contained around 1.3 mL of agent with up to $1.2 \times 10^{10}$ microbubbles (mean diameters of 1.1–3.3 μm with 98% being less than 10 μm), and about 150 μL/mL of octafluoropropane (i.e., $C_3F_8$).[23]

## Ultrasound Imaging

Ultrasound scanning was performed by an experienced sonographer or physician at each site. A modified Logiq 9 scanner (GE Healthcare, Waukesha, WI) was used with a 4D10L probe in 2D grayscale ultrasound, 2D power Doppler imaging (PDI), 3D HI, and 3D SHI modes prior to the clinically indicated biopsy.[21,22] Cine clips in 2D and 3D (i.e., image volumes) were acquired as well as radiofrequency (RF) data from 3D HI (transmitting at 5.0 MHz and receiving at 10.0 MHz using a pulse inversion technique) and 3D SHI (transmitting at 5.8 MHz and receiving at 2.9 MHz using pulse inversion).[17] These transmit and receive frequencies were optimized for use with Definity based on testing in previous studies.[17,18] The mechanical index (MI) at maximum transmit settings was measured as 0.36 for 3D HI (peak negative pressure of 0.80 MPa) and 0.33 (peak negative pressure of 0.79 MPa) for 3D SHI using a calibrated, 0.5 mm needle hydrophone (Precision Acoustics, Dorchester, Dorset, UK).

The target lesion was located with grayscale ultrasound and the maximum diameter was measured. Next, baseline 2D grayscale and 2D PDI cine clips (optimized on an individual basis according to good scanning practices) were acquired by manually sweeping across the entire lesion. Prior to acquiring 3D volumes, the imaging parameters (gain, depth, output power, etc.) were optimized for each subject (based on previous *in vitro* and pre-clinical animal imaging studies[17,18]) to allow visualization of the entire lesion with good contrast-to-tissue signal ratio. The volume angle was set to 19 degrees, which produced volume rates of 1.1 to 3.0 Hz (depending on lesion size). Contrast agent dosages were selected based on previous imaging experience by our group for each of the contrast modes.[13,18] For 3D HI, 0.25 mL of Definity was administered IV via a peripheral vein (typically the antecubital vein) followed by a 10 mL saline flush and then 3D HI volumes were acquired until sufficient contrast agent washout was observed (typically around 60 s). After waiting 10 minutes (to avoid any cumulative effect of the contrast agent and to ensure a return to baseline conditions) a second contrast bolus injection (20 μL/kg up to a maximum of 1.25 mL and afterward a 10 mL saline flush) was administrated for collecting 3D SHI volumes. Following the second ultrasound contrast agent injection, participants were monitored for 30 minutes before proceeding to their clinically indicated biopsy and the final histopathological assessment, which served as the reference standard for this study.

## Qualitative Assessments

Evaluation of the ultrasound clips and volumes was performed independently and off-line by five experienced radiologists blinded to the mammographic and pathological findings. Two readers assessed the data at each site (AS & AW at TJU and HOF & RFM at UCSD), while one radiologist evaluated all the cases across both sites (CWP selected due to her experience with breast SHI[13,14]). The 3D HI and 3D SHI volumes were visualized using a proprietary software 4DView (GE Medical Systems, Zipf, Austria). This software allowed the volumes to be viewed and manipulated as a function of time in 3D space or as individual 2D imaging planes (Figure 1A-D). Ultrasound diagnosis was scored based on a 7-point BIRADS scale: 1) no lesion seen or no findings, 2) benign, 3) probably benign, 4a) low suspicion of malignancy, 4b) intermediate suspicion of malignancy, 4c) moderate suspicion of malignancy, and 5) high suspicion of malignancy.[24]

The ultrasound diagnostic criteria were evaluated for each patient as follows: grayscale ultrasound; grayscale and PDI (baseline); and baseline and contrast-enhanced 3D volumetric clip randomized to either HI or SHI. After a waiting period of at least 6 weeks to minimize bias, readers were presented with baseline imaging clips and the remaining 3D HI or SHI volume. While this may have introduced some bias from pre- to post-contrast results, it was considered the more realistic approach to how contrast-enhanced ultrasound imaging (CEUS) is being used in clinical practice. Finally, SoC imaging (mammogram and/or ultrasound) was read by a radiologist as part of the patient's clinical assessment and evaluated using the BIRADS scale.[24]

All imaging variables collected were compared to all histopathological variables. The pre- and post-contrast ultrasound diagnostic criteria included: overall diagnosis; diagnostic confidence (in %), the size of the lesion (in mm); degree of enhancement (none, mild, good, or excellent); degree of vascularity (avascular, mild, moderate, highly focused, or highly diffuse); vascular morphology (none, in the lesion, immediately adjacent to the lesion, or diffusively surrounding the lesion); and vessel anastomoses (present or absent).

## Quantitative Assessments

Custom image processing tools were built using MATLAB (The Mathworks Inc., Natick, MA) to perform quantitative analyses as described in our previous work.[21,22] Briefly, lesions that demonstrated contrast-enhanced flow in 3D HI or SHI modes were identified by a radiologist and an ultrasound physicist in consensus (PM & AS) in 4DView and time intensity curves (TIC) calculated from the RF data across all 2D slices making up a 3D volume resulting in a single 3D TIC volume. Subsequently, these 3D TIC volumes were used to generate vascular heterogeneity (i.e., the distribution of vascularity within a volume), perfusion (PER) and area under the curve (AUC) or blood volume maps in the central, and peripheral regions of the lesion as well as the ratio within these two regions.[21,22] The central region was defined as the inner two-thirds of the entire tumor, while the remainder, including 2 mm around the lesion boundary constituted the peripheral region. A detailed description of the complete processing algorithm can be found elsewhere.[21,22]

## Statistical Analysis

Diagnostic accuracy, optimal sensitivity, and specificity for the four ultrasound imaging modes and SoC imaging was assessed with ROC and reverse, step-wise logistical regression analyses (individually as well as in combination with each other and with the quantitative TIC parameters) using histopathological biopsy results as the reference standard.[25,26] Differences between ROC curves were tested by computing Mann–Whitney statistics, while the $\kappa$-statistic was calculated for inter-reader agreement. Imaging judgments on diagnoses and characteristics of vascularity for the different modalities were compared (using two-way tests) to each other and to the histopathological results using t-tests or Wilcoxon sign rank tests. Statistical analyses were performed using Stata version 15.1 (Stata Corp LLC, College Station, TX) with a *P*-value of .05 or lower being considered statistically significant.

# Results

## Patient and Lesion Characteristics

The study enrolled 236 subjects, but image data were only available for 219 cases (56 at UCSD and 163 at TJU; average age 51 ± 13 years), due to technical failures with the ultrasound scanner ($N = 9$) and lack of IV access ($N = 8$). The 219 subjects that were successfully scanned were almost evenly split between Caucasian women (108 or 49%) and African-American women (97 or 44%), while 14 were of Asian descent (6%). There were 15 Hispanic women (7%) in this study.

Histopathology identified 164 lesions as benign (164/219, 75%) and 55 as malignant (55/219, 25%). Among the malignant lesions, invasive ductal carcinomas were the most common (42/55, 76%), while fibroadenomas were the most frequent benign lesion sub-type (51/164, 31%). Other lesion types encountered in this study are listed in Table 2. Finally, while malignant lesions were almost identical in size to benign lesions (13.5 ± 8.7 mm vs 13.2 ± 0.6 mm; $P = .83$), the average age of the women with a malignant lesion was significantly greater than that of women with benign lesions (58 ± 12 years vs 48 ± 13 years), $P < .0001$).

Contrast-enhanced flow was identified in 83 lesions with 3D SHI mode, which was similar to the vascularity seen with PDI (83 vs. 93 lesions; $P = .52$), but significantly greater than number of vascular lesions observed in 3D HI mode (83 vs. 8 lesions; $P < .0001$).[21,22] Hence, no additional quantitative processing and analysis were performed on these 3D HI cases.[21,22]

## Imaging Findings

An example of ultrasound imaging in a 68-year-old woman with a 1.93 by 1.49 cm invasive ductal carcinoma (ER and PR negative and HER-2 positive with a Ki-67 expression of 36%) is shown in Figure 1A-D. The ability to view multiple individual 2D imaging planes across the lesion volume (and as a function of time) in 4DView is demonstrated in Figure 1C and D. Hence, readers were able to identify regions of vascularity in 2D and 3D, which combined with the anatomical information of grayscale ultrasound (cf., Figure 1A) allowed them to characterize the breast mass.

The area under the individual ROC curves ($A_z$) for the diagnosis of breast cancer based on all 219 cases was 0.83, 0.82, 0.85, and 0.82 for grayscale ultrasound, PDI, 3D HI, and 3D SHI, respectively ($P = 0.31$; Figure 2A). For SoC imaging, the $A_z$ was 0.72, which was statistically significantly lower than that of all the ultrasound modes ($P < .03$). Very similar results were achieved in the subset of lesions that demonstrated contrast-enhanced flow ($A_z$'s of 0.82–0.83; $P = .84$; Figure 2B). The optimal sensitivities and specificities derived from Figure 2A and B were 78 to 84% and 69 to 83%, respectively, for the ultrasound modes as well as 58% and 68% for SoC imaging (i.e., mammography and/or ultrasound).

The diagnostic accuracy (i.e., $A_z$) for all five readers across the two sites is shown in Tables 3 and 4. There was no consistent improvement in diagnostic accuracy with volumetric contrast-enhanced HI or SHI. Out of the five readers, three saw an increase in diagnostic

confidence with 3D SHI on the order of 3 to 6% ($P < .041$), while two did not ($P > .11$). Inter-reader agreements were low to medium ($0.01 < \kappa < 0.52$). Overall, 3D SHI depicted more anastomoses, more vascularity, and a more diffuse vascular pattern than 3D HI ($P < .021$), but both CEUS modes did worse than 2D PDI ($P < .001$). Moreover, there were no differences for any of the vascularity assessments by any of the ultrasound modes when compared grouped by pathology ($P > .27$). Very similar results were achieved when the data were analyzed split by readers (not shown for brevity); although lesion vascularity did differentiate between malignant and benign lesions for two readers (one from each site; $P < .042$) the other two readers observed no such separation ($P > .09$).

### Comparison of Imaging Modalities and Quantitative Parameters

Reverse, step-wise, logistical regression techniques were used to combine the four ultrasound imaging modes (i.e., grayscale, PDI, 3D HI, and 3D SHI) and SoC imaging both overall as well as for readers split by site and in the subset of cases with contrast-enhanced flow. However, the only indication of synergy was in the overall data set where SoC imaging (mammography and/or ultrasound), grayscale ultrasound, and 3D HI combined for an Az of 0.88. All other logistical models reduced to just a single imaging mode (i.e., no synergistic improvements).

Finally, the ability to improve the characterization of the breast lesions identified with contrast-enhanced flow based on combining clinical reads and the vascular heterogeneity, PER or AUC parametric maps were determined. The quantitative parameters from the central and peripheral zones of the lesion as well as a ratio of these two regions were included in logistic models together with the readers' assessments. No single model was optimal for all five readers, but the best all-round results were achieved by combining the heterogeneity ratio with the central SHI PER parameter and the grayscale ultrasound evaluations (Figure 3). Diagnostic accuracies (i.e., $A_z$ values) for all five readers across the two sites ranged from 0.90 to 0.91 overall to 0.93, 0.97, and 1.00 (however, this last perfect result was based on only 18 cases with contrast-enhanced flow scanned at UCSD).

## Discussion

This multi-center study investigated the ability of 3D CEUS to characterize suspicious breast lesions using the clinical assessments of radiologists on their own or in combination with quantitative vascular parameters derived from 3D SHI compared to SoC imaging (mammography and/or ultrasound) and histopathology (the reference). Overall, the four ultrasound modes achieved accuracies of 82 to 85%, which was significantly better than SoC imaging (72%; $P < .03$; cf., Figure 2). Volumetric 3D SHI increased diagnostic confidence by 3 to 6% ($P < .05$) for 3 out of 5 readers, but inter-reader agreements were low to medium ($0.01 < \kappa < 0.52$).

Logistical regression analyses found only limited synergy between individual imaging modes (i.e., between grayscale, PDI, 3D HI, 3D SHI, and SoC imaging). However, in the sub-set of cases with quantitative parametric vascular data (i.e., the 83 breast lesions identified with contrast-enhanced flow), the best all-round results were achieved by combining the heterogeneity ratio with the central SHI PER parameter (i.e., functional

information), and the grayscale ultrasound evaluations (i.e., anatomical information). The overall $A_z$ reached 0.91, with 0.93 and 0.97 attained at TJU as well as 0.90 and 1.00 achieved at UCSD (the latter most likely influenced by the small number of cases; $N = 18$). These results are excellent (cf., Figure 3) and better than the accuracies obtained by the quantitative parameters alone (up to 0.90).[21,22]

The use of 3D CEUS as a tool for evaluating the structural and functional features of breast lesions is also supported by Chen and co-workers who showed significant differences in peripheral vessel characteristics between benign and malignant breast lesions using 3D contrast ultrasound.[27] Moreover, two recent meta-analyses of CEUS for characterizing breast lesions reported pooled summary ROC $A_z$ values of 0.92 and 0.95,[28,29] which are very similar to the results of this study.

As previously established, 3D SHI was considerably better at detecting vascular flow in these breast lesions compared to 3D HI.[22] In addition, SHI depicted more anastomoses and vascularity than HI ($P < .021$), but there were no differences when assessed by pathology ($P > .27$). As discussed in detail elsewhere, we attribute the poor performance of 3D HI to a number of factors, including low HI contrast dose (although dosages were selected based on previously reported work[17,30]), insufficient acoustic power output, and the transducer's reduced sensitivity in the CEUS modes or most likely a combination of all of these factors.[21,22]

Diagnosing breast lesions with CEUS has been studied for over 25 years, since conventional Doppler techniques lack the sensitivity to image vessels much below 200 μm in diameter whereas CEUS can detect signals in neovessels an order of magnitude smaller (down to 20–39 μm).[6,7,31] However, there are other ultrasound techniques capable of providing functional information on breast lesions such as shear wave elastography (SWE) and, more recently, (non-contrast) microvascular flow imaging modes.[4,5,28] A recent meta-analysis directly compared CEUS and SWE for characterizing breast lesions and reported an odds ratio of 27.14 in favor of CEUS.[28] Xiao and colleagues compared microvascular imaging and CEUS in breast imaging and found very similar performances ($A_z$ of 0.88 and 0.92, respectively; $P = .13$).[32] The diagnostic accuracy of breast microvascular imaging was reported to be 0.87 in a meta-analysis of over 2000 breast masses.[33] There may be synergy in combining CEUS and microvascular imaging directly for detecting breast cancer, but this possibility awaits future investigations.

It is important to note the limitations of this study. Only one overall reader evaluated all 219 cases. Nonetheless, since 74% of the cases (163 out of 219 women) were enrolled at one site (TJU), we feel that the reproducibility was reasonably well established by comparing the three readers at that site (unfortunately as medium at best). Moreover, our study may have been biased from the pre- to post-contrast assessments, because of the order of the reading (although this is how CEUS is being used in clinical practice). Less than 40% of the breast lesions imaged in this study were vascular, which was surprising. A combination of low contrast agent dosages and limited probe sensitivity in the CEUS modes are most likely the cause. Advances in transducer technology and the development of matrix arrays for 3D imaging may overcome these limitations in future clinical trials. Alternatively, further image

(or rather volume) processing using a maximum intensity projection algorithm may improve results.[14] However, the raw image data are saved at a low resolution (usually around 40 × 50 pixels per 2D image slice), which makes this a technically challenging proposition.[22]

In conclusion, this prospective, multi-center study assessed the ability of 3D HI and 3D SHI to characterize suspicious breast lesions using clinical assessments and quantitative parameters. Results were compared to conventional ultrasound and mammography and although the ultrasound modes did better than SoC imaging 3D CEUS was not in and of itself better than the other ultrasound modes. However, when anatomical information from grayscale imaging was combined with functional vascular data from quantitative 3D SHI parameters the ability to accurately characterize breast lesions improved markedly (with $A_z$ reaching 0.97). Hence, clinical reads and quantitative 3D SHI parameters together may provide a new, accurate, and patient-friendly imaging tool for the diagnosis of suspicious breast lesions.

## Acknowledgments

We gratefully acknowledge the efforts of the many research coordinators who helped recruit subjects for this trial. This work was supported by National Institutes of Health Grant R01 CA140338, U.S. Army Medical Research Material Command Grant W81XWH-11-1-0630, and by Lantheus Medical Imaging, N. Billerica, MA, which supplied the ultrasound contrast agent Definity.

FF: Equipment, contrast agent, and grants support from GE Healthcare. Equipment and grant support from Canon Medical Systems America. Equipment and grant support from the Butterfly Network. Drug support and speaker honorarium from Lantheus Medical Imaging. Equipment support from Siemens Healthineers. Drug support from Bracco. Consultant for Samumed and Exact Therapeutics. KW: Employee of GE. JRE: Equipment, contrast agent, and grants support from GE Healthcare. Drug support and speaker honorarium from Lantheus Medical Imaging. Equipment support from Siemens Healthineers. Royalties from Elsevier. Others have reported no disclosures.

## Abbreviations

| | |
|---|---|
| **AUC** | area under the curve |
| **CEUS** | contrast-enhanced ultrasound imaging |
| **FDA** | Food and Drug Administration |
| **HI** | harmonic imaging |
| **IRB** | Institutional Review Board |
| **IV** | intravenous |
| **MI** | mechanical index |
| **PDI** | power Doppler imaging |
| **PER** | perfusion |
| **RF** | radiofrequency |
| **ROC** | receiver operating characteristic |
| **SHI** | subharmonic imaging |

| | |
|---|---|
| **SoC** | standard of care |
| **TIC** | time intensity curves |
| **TJU** | Thomas Jefferson University |
| **UCSD** | University of California–San Diego |

## References


1. Siegel RL, Miller KD, Fuchs HE, Jemal A. Cancer statistics, 2021. CA Cancer J Clin 2018; 71:7–33.
2. Heer E, Harper A, Escandor N, Sung H, McCormack V, Fidler-Benaoudia MM. Global burden and trends in premenopausal and postmenopausal breast cancer: a population-based study. Lancet Glob Health 2020; 8:e1027–e1037. [PubMed: 32710860]
3. Duffy SW, Tabár L, Yen AM, et al. Mammography screening reduces rates of advanced and fatal breast cancers: results in 549,091 women. Cancer 2020; 126:2971–2979. [PubMed: 32390151]
4. Bicchierai G, Di Naro F, De Benedetto D, et al. A review of breast imaging for timely diagnosis of disease. J Int J Environ Res Public Health 2021; 18:5509. [PubMed: 34063854]
5. Park AY, Seo BK, Han MR. Breast ultrasound microvascular imaging and radiogenomics. Korean J Radiol 2021; 22:677–687. [PubMed: 33569931]
6. Lyshchik A Specialty Imaging: Fundamentals of CEUS. Amsterdam, The Netherlands: Elsevier; 2019.
7. Forsberg F, Kuruvilla B, Pascua MB, et al. Comparing contrast-enhanced color flow imaging and pathological measures of breast lesion vascularity. Ultrasound Med Biol 2008; 34:1365–1372. [PubMed: 18436369]
8. Forsberg F, Gupta I, Machado P, et al. Contrast-enhanced subharmonic aided pressure estimation (SHAPE) using ultrasound imaging with a focus on identifying portal hypertension. J Vis Exp 2020; 166:10.3791/62050.
9. Shankar PM, Krishna PD, Newhouse VL. Advantage of subharmonic over second harmonic backscatter for contrast-to-tissue echo enhancement. Ultrasound Med Biol 1998; 24:395–399. [PubMed: 9587994]
10. Forsberg F, Shi WT, Goldberg BB. Subharmonic imaging of contrast agents. Ultrasonics 2000; 38:93–98. [PubMed: 10829636]
11. Chomas J, Dayton P, May D, Ferrara K. Nondestructive subharmonic imaging. IEEE Trans Ultrason Ferroelectr Freq Control 2002; 49:883–892. [PubMed: 12152942]
12. Goertz DE, Frijlink ME, Tempel D, et al. Subharmonic contrast intravascular ultrasound for vasa vasorum imaging. Ultrasound Med Biol 2007; 33:1859–1872. [PubMed: 17683850]
13. Forsberg F, Piccoli CW, Merton DA, et al. Breast lesions: imaging with contrast-enhanced subharmonic US—initial experience. Radiology 2007; 244:718–726. [PubMed: 17690324]
14. Dave JK, Forsberg F, Fernandes S, et al. Static and dynamic cumulative maximum intensity display mode for subharmonic breast imaging: a comparative study with mammographic and conventional ultrasound techniques. J UltrasoundMed 2010; 29:1177–1185.
15. Eisenbrey JR, Dave JK, Merton DA, Palazzo JP, Hall AL, Forsberg F. Parametric imaging using subharmonic signals from ultrasound contrast agents in patients with breast lesions. J Ultrasound Med 2011; 30:85–92. [PubMed: 21193708]
16. Faez T, Emmer M, Docter M, Sijl J, Versluis M, de Jong N. Characterizing the subharmonic response of phospholipid-coated microbubbles for carotid imaging. Ultrasound Med Biol 2011; 37:958–970. [PubMed: 21531498]
17. Eisenbrey JR Sridharan A, Machado P, et al. Three-dimensional subharmonic ultrasound imaging in vitro and in vivo. Acad Radiol 2012; 19:732–739. [PubMed: 22464198]
18. Sridharan A, Eisenbrey JR, Liu J-B, et al. Perfusion estimation using contrast-enhanced 3-dimensional subharmonic ultrasound imaging: an in vivo study. Invest Radiol 2013; 48:654–660. [PubMed: 23695085]

19. Kanbar E, Fouan D, Sennoga CA, Doinikov AA, Bouakaz A. Impact of filling gas on subharmonic emissions of phospholipid ultrasound contrast agents. Ultrasound Med Biol 2017; 43:1004–1015. [PubMed: 28214036]
20. Shekhar H, Rowan JS, Doyley MM. Combining subharmonic and ultraharmonic modes for intravascular ultrasound imaging: a preliminary evaluation. Ultrasound Med Biol 2017; 43:2725–2732. [PubMed: 28847499]
21. Sridharan A, Eisenbrey JR, Machado P, et al. Quantitative analysis of vascular heterogeneity in breast lesions using contrast-enhanced 3-D harmonic and subharmonic ultrasound imaging. IEEE Trans Ultrason Ferroelectr Freq Control 2015; 62:502–510. [PubMed: 25935933]
22. Sridharan A, Eisenbrey JR, Stanczak M, et al. Characterizing breast lesions using quantitative parametric 3D subharmonic imaging: a multicenter study. Acad Radiol 2020; 27:1065–1074. [PubMed: 31859210]
23. United States Food and Drug Administration. Definity package insert. https://www.accessdata.fda.gov/drugsatfda_docs/label/2011/021064s011lbl.pdf. Accessed July 26, 2021.
24. American College of Radiology. ACR BI-RADS Atlas. 5th ed. Reston, VA: American College of Radiology; 2013.
25. Metz CE. ROC methodology in radiologic imaging. Invest Radiol 1986; 21:720–733. [PubMed: 3095258]
26. Liu X Classification accuracy and cut point selection. Stat Med 2012; 31:2676–2686. [PubMed: 22307964]
27. Chen M, Wang WP, Jia WR, et al. Three-dimensional contrast-enhanced sonography in the assessment of breast tumor angiogenesis correlation with microvessel density and vascular endothelial growth factor expression. J Ultrasound Med 2014; 33:835–846. [PubMed: 24764339]
28. Huang R, Jiang L, Xu Y, et al. Comparative diagnostic accuracy of contrast-enhanced ultrasound and shear wave elastography in differentiating benign and malignant lesions: a network meta-analysis. Front Oncol 2019; 9:102–121. [PubMed: 30891425]
29. Li Q, Hu M, Chen Z, et al. Meta-analysis: contrast-enhanced ultrasound versus conventional ultrasound for differentiation of benign and malignant breast lesion. Ultrasound Med Biol 2018; 44: 919–929. [PubMed: 29530434]
30. Hoyt K, Umphrey H, Lockhart M, et al. Ultrasound imaging of breast tumor perfusion and neovascular morphology. Ultrasound Med Biol 2015; 41:2292–2302. [PubMed: 26116159]
31. Kedar RP, Cosgrove D, McCready VR, et al. Microbubble contrast agent for color Doppler US: effect on breast masses. Work in progress. Radiology 1996; 198:679–686. [PubMed: 8628854]
32. Xiao X, Chen X, Guan X, et al. Superb microvascular imaging in diagnosis of breast lesions: a comparative study with contrast-enhanced ultrasonographic microvascular imaging. Br J Radiol 2016; 89:1–8.
33. Zhong L, Wang C. Diagnostic accuracy of ultrasound superb microvascular imaging for breast tumor: a meta-analysis. Med Ultrason 2020; 22:313–318. [PubMed: 32898204]

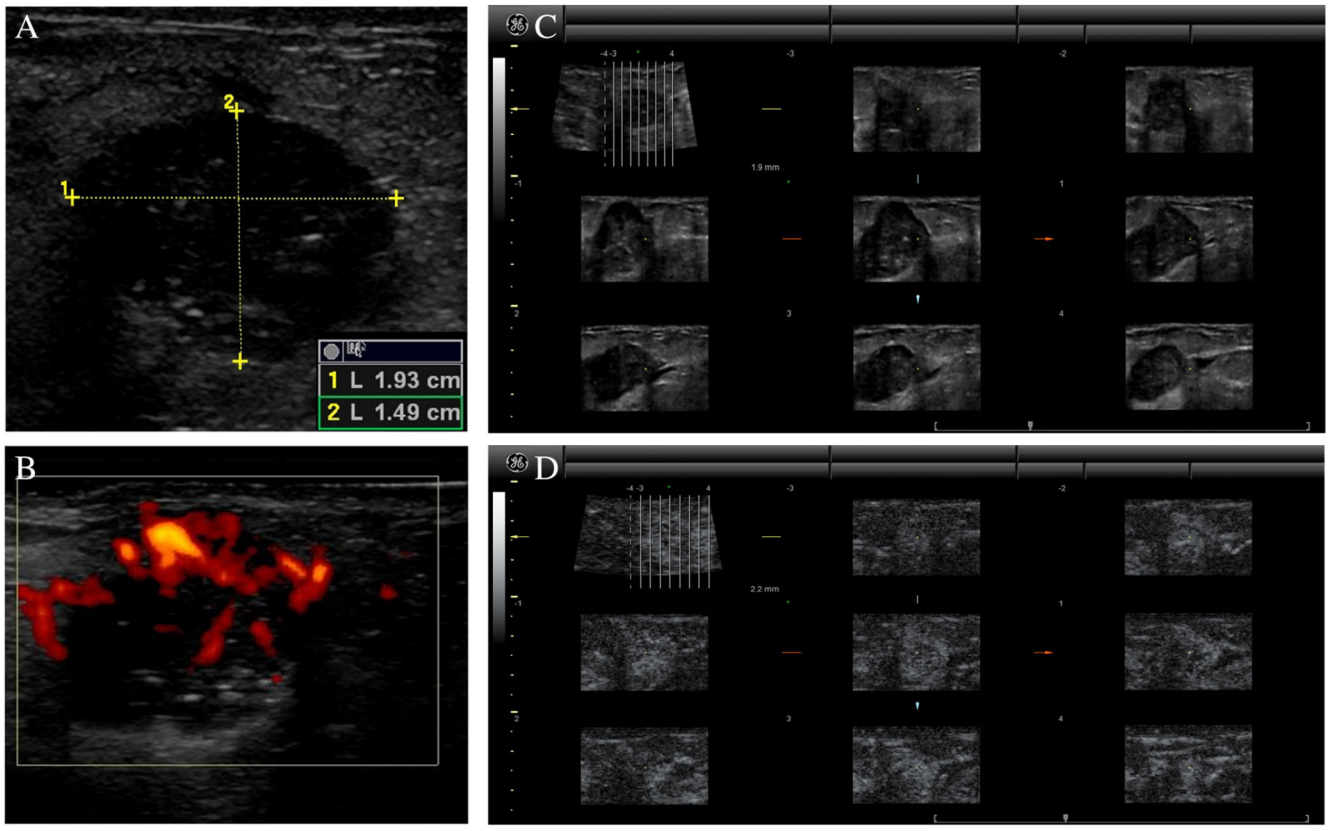


**Figure 1.**

Example of a 1.93 × 1.49 cm invasive ductal carcinoma imaged in a 68-year-old woman. **A,** Baseline grayscale imaging. **B,** Baseline PDI demonstrating marked vascularity throughout the lesion. **C,** Visualization of the lesion in 3D HI mode with contrast enhancement using 4DView. Multiple individual 2D imaging planes across the lesion volume (the slice separation was 2 mm) are shown. **D,** Visualization of the lesion in 3D SHI mode with contrast enhancement using 4DView. Notice the marked enhancement seen compared to the 3D HI images.

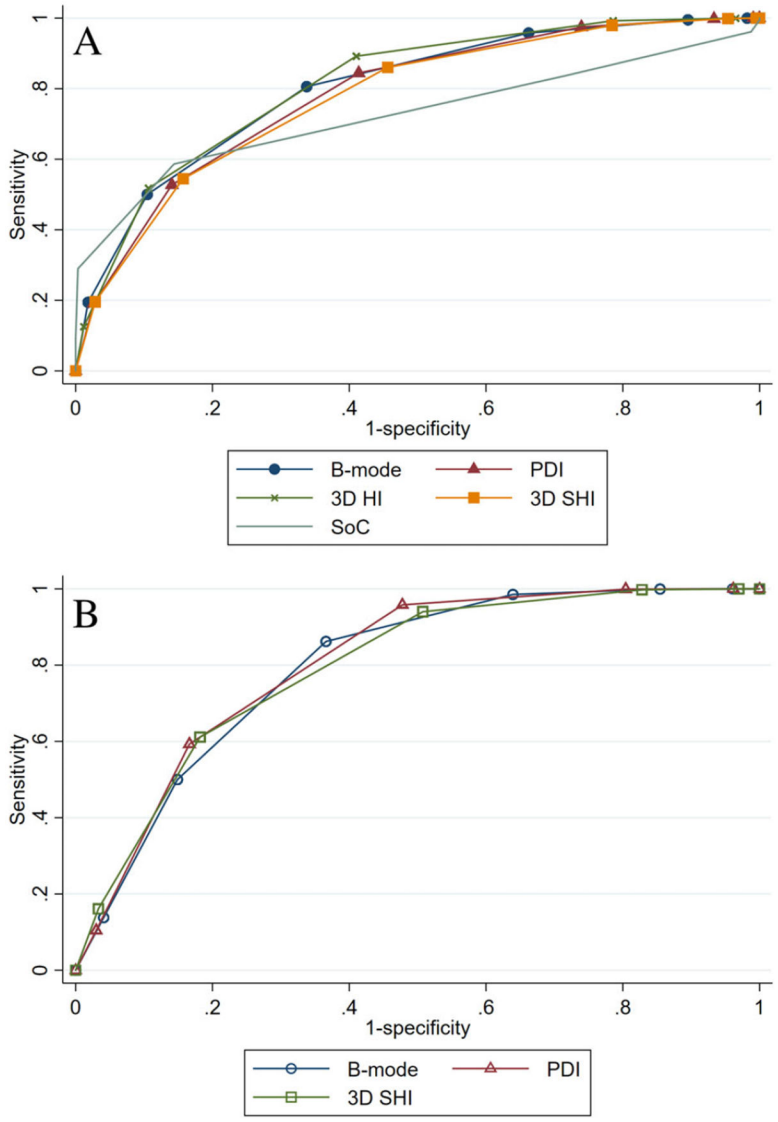


**Figure 2.**

Overall clinical assessments. **A,** ROC curves for grayscale ultrasound, PDI, 3D HI, and 3D SHI as well as SoC imaging (mammography and/or ultrasound) with $A_z$'s of 0.83, 0.82, 0.85, 0.82, and 0.72, respectively. The diagnostic accuracy of SoC imaging was significantly lower than those of the ultrasound modes ($P < .03$). **B,** ROC curves for the subset of lesions that demonstrated contrast-enhanced flow ($A_z$'s of 0.82–0.83).

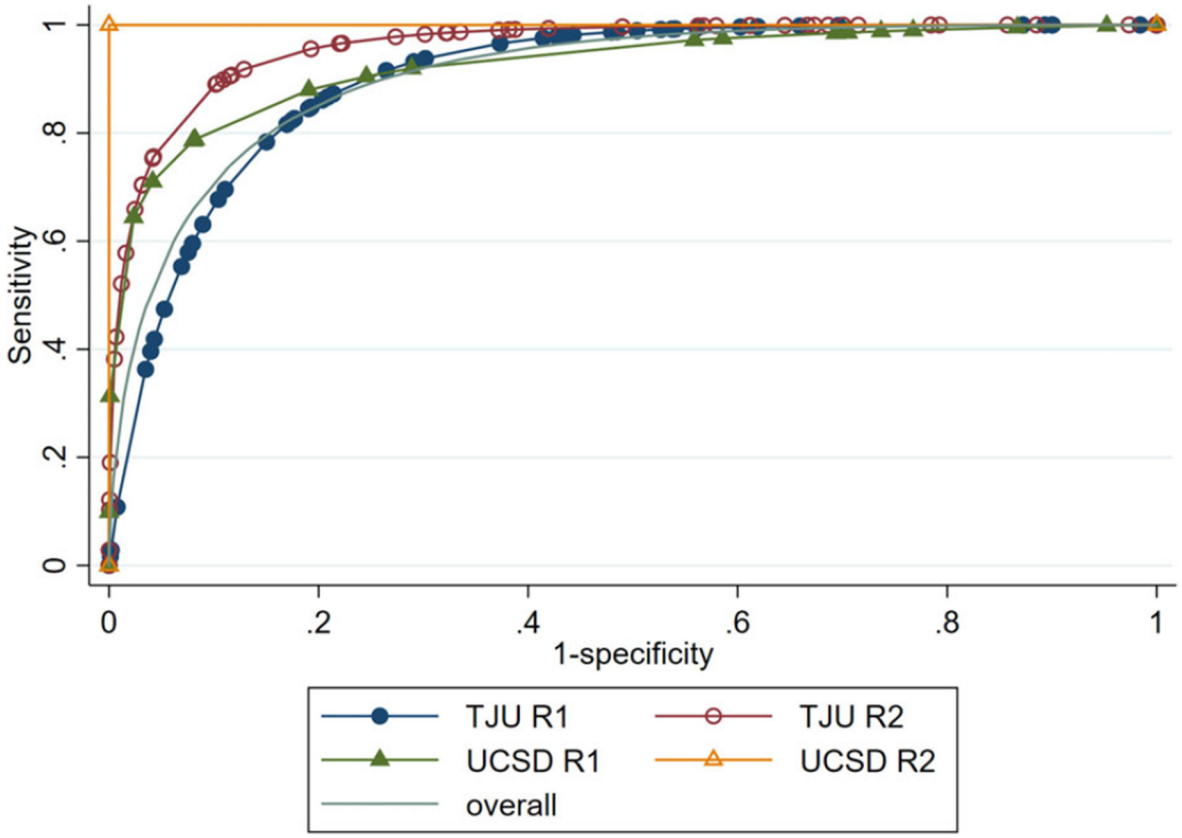


**Figure 3.**

ROC curves for the best regression model combining the heterogeneity ratio with the central SHI perfusion parameter and grayscale ultrasound evaluations split by reader. Diagnostic accuracies were 0.90 (UCSD reader1), 0.91 overall, 0.93 (TJU reader 1), 0.97 (TJU reader 2), and 1.00 (UCSD reader 2).

**Table 1.**

Inclusion and Exclusion Criteria

| Inclusion Criteria | Exclusion Criteria |
|---|---|
| Be a female scheduled for a breast biopsy of an indeterminate mass or region of abnormality | Clinically unstable cardiac disease (arrhythmias, uncontrolled congestive heart failure, pulmonary hypertension, etc.) |
| Be at least 21 years of age | Breast lesion is unequivocally a cyst by unenhanced grayscale imaging |
| Be medically stable | Pregnant or nursing |
| Have a negative pregnancy test if of child-bearing potential | Known contraindication to Definity contrast agent |
| Be able to understand the study and provide written consent | Medically unstable, seriously or terminally ill |
| | Excisional biopsy/lumpectomy of the area of interest within the past 6 weeks |

**Table 2.**

Lesion Subtypes in the Study

| | | Lesions | |
|---|---|---|---|
| | | **Number** | **Percent (%)** |
| Malignant (*N* = 55) | Invasive ductal carcinoma | 42 | 76 |
| | Invasive lobular carcinoma | 4 | 7 |
| | Invasive papillary carcinoma | 2 | 4 |
| | Ductal carcinoma *in situ* | 7 | 13 |
| Benign (*N* = 164) | Fibroadenoma | 51 | 31 |
| | Cysts | 31 | 19 |
| | Hyperplasia | 22 | 13 |
| | Lymph nodes | 14 | 9 |
| | Adenosis | 8 | 5 |
| | Intraductal papilloma | 3 | 2 |
| | Fibroepithelial lesion | 2 | 1 |
| | Fat | 4 | 2 |
| | Mastitis | 2 | 1 |
| | Other benign components | 27 | 16 |

**Table 3.**

Diagnostic accuracy ($A_z$) by readers (R1—R3) at TJU ($N$ = 163)

| | B-Mode | | PDI | | 3D HI | | 3D SHI | |
|---|---|---|---|---|---|---|---|---|
| | All | Flow | All | Flow | All | Flow[a] | All | Flow |
| R1 | 0.82 | 0.86 | 0.81 | 0.82 | 0.85 | — | 0.81 | 0.80 |
| R2 | 0.88 | 0.94 | 0.88 | 0.93 | 0.84 | — | 0.85 | 0.91 |
| R3 | 0.82 | 0.80 | 0.80 | 0.79 | 0.85 | — | 0.79 | 0.76 |

[a]The number of lesions identified with flow in 3D HI mode was too small for analysis.

**Table 4.**

Diagnostic Accuracy ($A_z$) by Readers (R1—R3) at UCSD ($N = 56$)

| | B-Mode | | PDI | | 3D HI | | 3D SHI | |
|---|---|---|---|---|---|---|---|---|
| | All | Flow | All | Flow | All | Flow[a] | All | Flow |
| R1 | 0.61 | 0.69 | 0.61 | 0.75 | 0.63 | — | 0.69 | 0.74 |
| R2 | 0.55 | 0.61 | 0.57 | 0.52 | 0.63 | — | 0.61 | 0.55 |
| R3 | 0.62 | 0.67 | 0.66 | 0.67 | 0.59 | — | 0.62 | 0.63 |

[a]The number of lesions identified with flow in 3D HI mode was too small for analysis.